ACERP: Vol. 6, No.2, (Spring 2020) 1-6

Advanced Ceramics Progress

Research Article

Journal Homepage: www.acerp.ir

Comparison of Semiconducting Behavior and Optical Properties of Oxyfluoride Glasses of SiO_2-Al_2O_3-BaF_2 and SiO_2-Al_2O_3-CaF_2 Systems

L. Farahinia [a], M. Rezvani [a] *, M. Rezazadeh [b]

[a] *Department of Materials Engineering, Faculty of Mechanical Engineering, University of Tabriz, Tabriz, Iran*
[b] *Department of Materials Engineering, Isfahan University of Technology, Isfahan , Iran*

PAPER INFO

Paper history:

Received 31 August 2019
Accepted in revised form 09 February 2020

Keywords:

Bandgap
Semiconductor Glass
Oxyfluoride

ABSTRACT

Amorphous semiconductors are materials with a brilliant prospect for a wide range of optical applications like solar cells, optical sensors, optical devices, and memories. The purpose of the present research was to study the semiconducting optical properties of SiO_2-Al_2O_3-CaF_2 and SiO_2-Al_2O_3-BaF_2 oxyfluoride glassy systems, which has been rarely studied from this point of view. The suitable compositions in the mentioned systems were chosen and melted in covered alumina crucibles at 1450˚C. Afterward, preheated stainless steel molds were used to shape the molten glasses. The absence of any crystallization peak in the XRD results indicated that the samples were amorphous. DTA patterns showed that the crystallization temperature of the fluoride phase is 693˚C for the glass containing BaF_2 (SAB), which is higher than the peak temperature (684˚C) for the glass with CaF_2 (SAC). DTA results were in accordance with density measurements, i. e., the density of the glass SAB (3.85 $g.cm^{-3}$) was higher than the glass SAC (2.70$g.cm^{-3}$). That is to say, BaF_2 presented a more continuous structure with lower amounts of dangling bonds. According to the UV-Vis spectra, sample SAB had higher absorption and smaller bandgap of the glass SAB (with a direct bandgap of 2.90 eV and indirect bandgap of 3.40 eV) indicated that it has better semiconducting behavior than sample SAC (with a direct bandgap of 3.07 eV and indirect bandgap of 3.60 eV). This increment of the semiconducting behavior is attributed to the more continuous structure of the glass SAB. Urbach energy, which is an indicator of disorder degree of structure, was 0.20 and 0.32eV for SAB and SAC, respectively. Therefore, the lower Urbach energy of SAB glass confirmed the higher structure order of it.

1. INTRODUCTION

When fluoride glasses were invented by Poulain et al. (1975) [1], nobody could imagine that these glasses would become the base of photonic glasses such as ZBLAN. The presence of heavy metal fluorides was the reason why they demonstrated unique optical characteristics like the preparation of fibers [2]. In fact, they have a very high position in optics considering the lower phonon energy of fluoride glasses (500 cm^{-1}) compared to oxide glasses [3]. Despite their low phonon energy, fluoride glasses encounter problems like weak thermal, chemical, and mechanical durability [4]. Hence, there were many attempts to solve the mentioned disadvantages, especially during the last decades. It has been shown that introducing oxygen to the network of fluoride glasses or adding fluorides to oxide melts accelerates crystallization. In case of adding high amounts of mentioned components, the outcome will be completely different. That is to say, if the percentage of oxygen gets high, as if it is one of the basic components, it can play the stabilizing role in fluoride glass [5]. A new concept emerged that entitled oxyfluoride glasses considering the entire mentioned above. Some amount of fluorine is substituted by oxygen in oxyfluoride glasses, which this leads to a more continuous glass network as well as higher stability [5].

The importance of oxyfluoride glasses arose from the crystallization possibility of them and resulting in transparent oxyfluoride glass-ceramics. For the first time, Ohwaki and Wang produced oxyfluoride glass-ceramics containing Er^{3+}/Yb^{3+}-doped $(Pb_x,Cd_{1-x})F_2$ nanocrystals [6]. They reported that the red emission of Er^{3+} ions has a higher intensity in the glass-ceramic sample than an amorphous one. This event was due to the effective energy transfer or cross-relaxation between Er^{3+} and Yb^{3+}

* Corresponding Author Email: m_rezvani@tabrizu.ac.ir (M. Rezvani)

https://doi.org/10.30501/acp.2020.105938

in crystallized samples, which was caused by the entrance of rare-earth ions into the low phonon energy-fluoride nanocrystals [6]. In other words, such kinds of glass-ceramics present both advantages of fluoride single crystals and oxide glasses [7]. After this achievement, Pb and Cd eliminated from oxyfluoride glasses and composition of glass-ceramics because of their environmental concerns [8]. Many substituents proposed by researchers like Dejneka who introduced oxyfluoride glass-ceramics containing LaF_3 nanocrystals. Although it was not toxic, the high cost of LaF_3 limited its applications and hindered its getting commercial [9]. Oxyfluoride glass-ceramics containing MF_2 (M=Ca, Ba, Sr) nanocrystals have received great attention during the last two decades as they are not toxic, they are economical, and have high solubility of rare-earth ions [8]. While a wide range of studies is devoted to optical semiconducting properties, luminescence, and up-conversion behavior of the base glass of MF_2 systems, there is not any comparison study between them. Therefore, the purpose of this study is to compare the optical semiconducting properties of two different MF_2 systems, i.e., SiO_2-Al_2O_3-CaF_2 and SiO_2-Al_2O_3-BaF_2. For this purpose, the optical bandgap and Urbach energy calculations were implemented after preparing transparent glasses.

2. EXPERIMENTAL PROCEDURE

High purity of raw materials were weighed and homogenized after choosing a suitable composition in each of the SiO_2-Al_2O_3-BaF_2 and SiO_2-Al_2O_3-CaF_2 systems (Table 1). K_2O was also used in the composition of glasses as a flux agent. Sb_2O_3 and As_2O_3 were added to batches to make bubble-free samples. Afterward, 50g of batches were melted in covered alumina crucibles in the electrical furnace at 1450˚C for 1hr.

TABLE 1. Chemical compositions of glasses in SiO_2-Al_2O_3- BaF_2 and SiO_2- Al_2O_3- BaF_2 systems (molar ratio)

Composition / Sample code	SiO_2	Al_2O_3	BaF_2	CaF_2	K_2O
SAB	50	20	30	-	5
SAC	50	20	-	30	5

Preheated steel molds (at 500 ˚C) were used to shape disc-like samples. Annealing process at 500 ˚C for 1 hour was applied for releasing internal stresses of shaped glasses.

Siemens D-500 system was used to record XRD patterns (Cu-Kα with the wavelength of 1.54Å). The scanning rate was chosen 0.5˚.min^{-1} to identify the crystalline phases or amorphous nature of specimens. Crystallization peak temperatures of glasses were obtained from DTA curves, which are obtained using DTG-60AH Shimadzu equipment with a heating rate of 10˚.min^{-1}. The density of samples was measured by the Archimedes standard method as follows:

$$D = \frac{W_1}{W_1 - W_2} \quad (1)$$

Where W_1 and W_2 are weights of the sample in air and water, respectively. Moreover, the molar volume is calculable using Equation 2:

$$V_m = \sum \frac{M_i}{D} \quad (2)$$

in Equation 2, M_i stands for molar mass, which is equal to:

$$M_i = C_i A_i \quad (3)$$

Where C_i and A_i are the molar concentration and the molecular weight of the ith component, respectively.
Moreover, the microhardness of samples is measured by Vickers micro-hardness equipment (HV-1000Z of PACE Technologies). For this purpose, the indentor was applied by the pressure of 1 N for 15 s.
The optical direct and indirect bandgap energy, Urbach tailing energy, and UV-Vis spectra of glasses were obtained by UV- Vis Shimadzu 1700 spectrophotometer to investigate the transparency. Accordingly, Tauc plots were drawn using their spectra and direct/indirect bandgap energy of samples were calculated. Urbach energy was also obtainable from Ln(α) vs. hυ diagrams and considering their slopes.

3. RESULTS AND DISCUSSION

3.1. Crystallization behavior of SAB and SAC glasses

DTA curves of SAB and SAC oxyfluoride glasses are presented in Figure 1. Similar to the DTA results of typical oxyfluoride glasses, initially, exothermic peaks are related to the crystallization of BaF_2 and CaF_2 nanocrystals in SAB and SAC glasses, respectively [10]. Furthermore, $BaAl_2Si_2O_8$ precipitates in BaF_2 containing glasses and $CaAl_2Si_2O_8$ (anorthite) in CaF_2-based glasses at the second exothermic peak temperatures. Precipitating of these aluminosilicate phases at second peak temperature is known as the crystallization of residual glassy matrixes [11, 12].

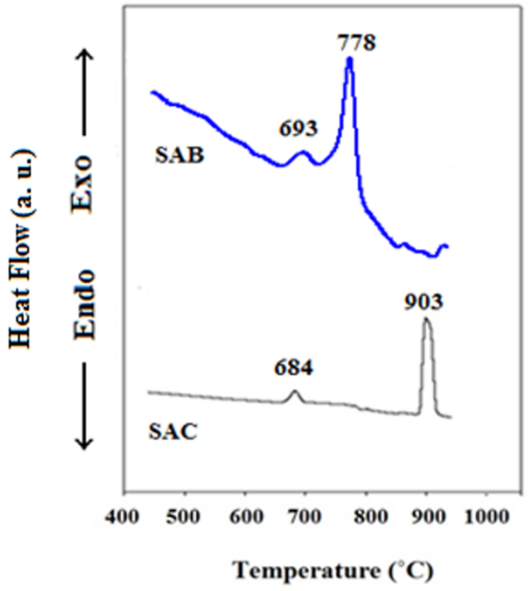

Figure 1. DTA curves of SAB and SAC samples

It is observable from Fig. 1 that the crystallization peak temperature of CaF_2 (684 ˚C) in the SAC sample is lower than BaF_2 (693 ˚C) in SAB glass. Factually, the crystallization of CaF_2 is somehow easier than BaF_2 in oxyfluoride glasses, which is probably due to the bond strengths in glasses, i.e., the crystallization accompanies the active dissociation of atomic bonds. Since energy of Ca-F and Ca-O bonds (523 and 351 KJ.mol^{-1}, respectively) are lower in comparison with Ba-F and Ba-O bonds (581 and 548KJ.mol^{-1}, respectively), lower activation energy are needed for crystallization of SAC glass [13]. Higher hardness of sample SAB is ascribed to the stronger bond energy of Ba-F and Ba-O compared to Ca-F and Ca-O bonds. On the other hand, two exothermic peaks in the DTA curve of the SAB sample are too close to each other, and the crystallization of BaF_2 overlaps with the crystallization of the glass matrix. Hence, the preparation of glass-ceramics containing only BaF_2 nanocrystals from SiO_2- Al_2O_3- BaF_2 glasses is difficult, which sounds to be easier for the SAC sample to be crystallized as glass-ceramics containing only CaF_2 nanocrystals [13].

Figure 2(a) represents the XRD patterns of SAB and SAC glasses. The absence of any crystallization peak and the presence of broad humps indicate the amorphous nature of samples. Furthermore, two humps in XRD patterns of each sample show the possibility of precipitation of two different crystalline phases, which is in accordance with DTA results.

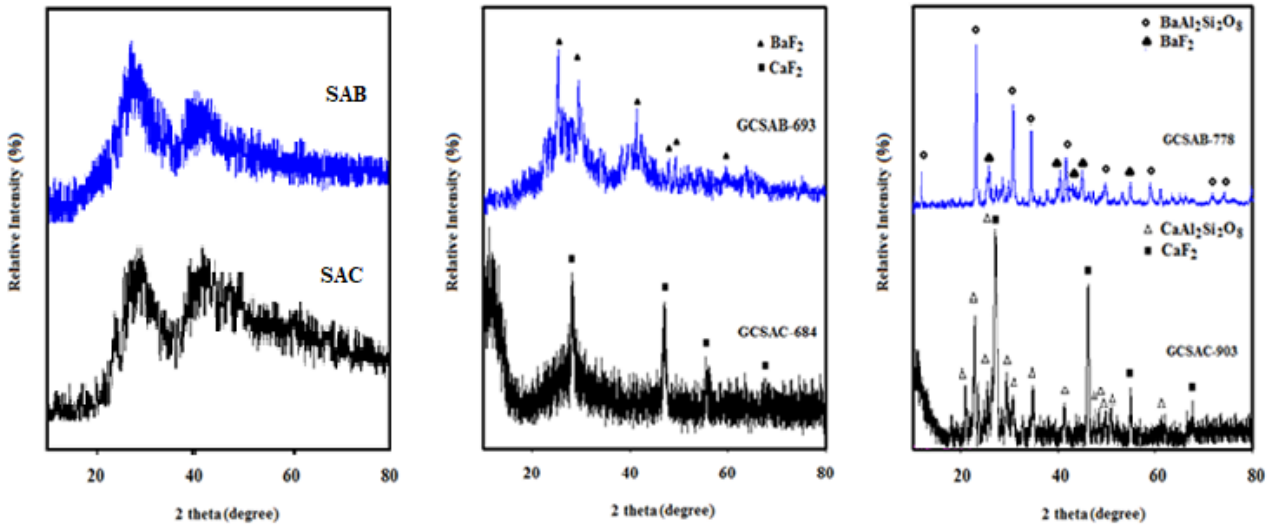

(a) **(b)** **(c)**

Figure 2. XRD patterns of **(a)** glasses and samples heat-treated at their **(b)** first and **(c)** second peak temperatures

Figure 2(b) and (c) exhibit the XRD results of SAB and SAC samples crystallized at their first and second DTA peak temperatures. According to these patterns, the only crystalline phase in glass-ceramics obtained at first peak temperatures (GCSAC-684 and GCSAB-693) are CaF_2 (JCPDS No. 35-0816) and BaF_2 (JCPDS No. 4-452). As claimed above, heat-treating at second peak temperature resulted in the crystallization of aluminosilicate phases in parallel with fluoride crystals (Fig. 2(c)). BaF_2 peaks in the XRD pattern of GCSAB-693 are broader than CaF_2 peaks of GCSAC-684. In other words, the movement of fluoride ions through the barriers around the fluoride crystallites that are Al_2O_3 and SiO_2 – riched layers, gets difficult and no more growth happens for nanocrystals of BaF_2 owing to the diffusion-controlled crystallization mechanism of both CaF_2 and BaF_2 oxyfluoride glasses

and more stronger atomic bonds in BaF_2 containing oxyfluorides [14,15]. As a consequence, the mean crystal size of nanocrystals is 10 and 19nm using the Scherrer equation for samples GCSAB-693 and GCSAC-684, respectively.

3.2. UV-Vis spectra and bandgap study

Figure 3 shows the UV-Vid spectra of specimens. The absorbance of SAB is higher than SAC, and its absorption edge is shifted to longer wavelengths. It should be noticed that the absorbance and absorption edge are affected by the bonds in glass network structure in all glassy materials [16]. In fact, only electrons of outer layers of materials can be excited and the result is absorption in the case of the incidence of a wavelength within the UV-Vis region. As discussed in the previous section, the bonds in SAB glass are much stronger than bonds in SAC glass. Therefore, there are less weak and dangling bonds in SAB, and the mean free path increases for this glass, and subsequently, its bandgap should be smaller [17]. To justify this claim, Tauc plots of both SAC and SAB glasses are presented in Fig. 4. According to Mott and Davis [18], the absorption coefficient (α) of an amorphous solid is related to the energy of the incident photon (hυ) and optical bandgap (E_g^{opt}). They proposed an equation for such behavior (Equation 4).

$$\alpha = \beta^{2} \frac{(h\upsilon - E_g^{opt})}{h\upsilon} \quad (4)$$

where β is a constant value representing the residual band constant, which it is dependent on the refractive index of the sample. Moreover, according to indirect allowed, indirect forbidden, direct allowed, and direct forbidden transitions, the amount of n is 2, 3, 1/2, and 1/3, respectively [19]. Hence, based on the Tauc plots presented in Fig. 4, optical bandgap energy can be calculated. For this purpose, the intercept of the obtained linear part divided by its slope [19-21].

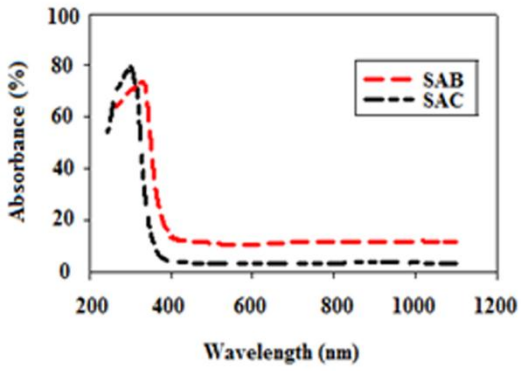

Figure 3. UV-Vis spectra of glasses

The calculated values for direct and indirect bandgaps (tabulated in Table 2) show that the bandgap energy of SAB is lower than the SAC sample, which proves the validity of the above-mentioned claim, i.e., SAB glass has a more continuous network with lower amounts of dangling bonds.

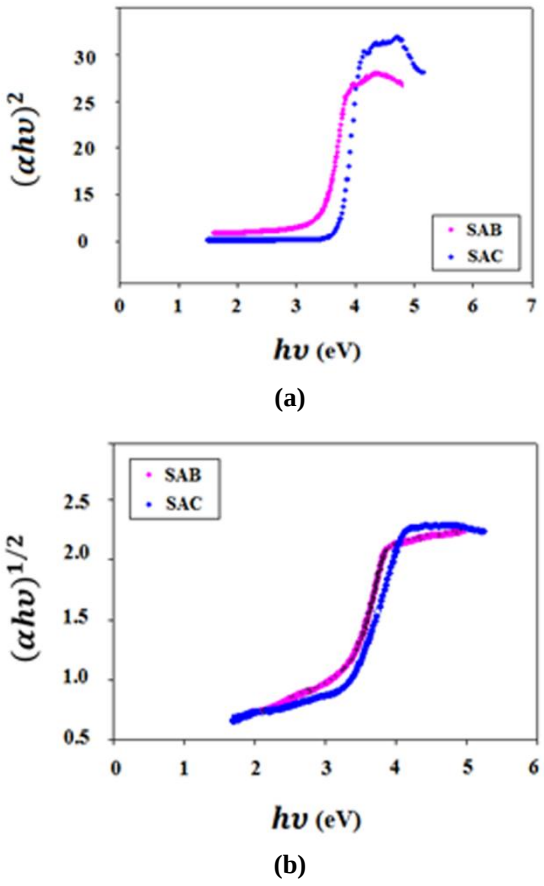

Figure 4. Tauc plots of **(a)** direct and **(b)** indirect bandgaps of SAC and SAB glasses

Additionally, the results of density measurements and molar volume calculations (also presented in Table 2) demonstrate that SAB has higher density and consequently lower V_m than SAC, which proves the more continuous structure.

TABLE 2. Some physical properties of SAC and SAB glasses

Sample Code	E_g Indirect (eV)	E_g Direct (eV)	E_U (eV)	V_m (cm^3/mol)	Hardness (MPa)	D (g/cm^3)
SAC	3.60	3.07	0.32	27.90	677.3	2.70
SAB	3.40	2.90	0.20	26.87	720.2	3.85

Short-range order in amorphous materials is the reason for weaker bonds between atoms and makes localized bond electrons in such atoms. These weak bonds result in tails in the bandgap and reduce the effective bandgap. However, the mobility of these electrons in tails is very hard and they do not play a role in the conduction of material. These tails are known as Urbach tails [22]. That is why the Urbach tail is considered as a degree of disorder in amorphous materials. Urbach energy (E_U) is obtainable using equation 5 and plotting diagrams of Ln(α) vs. hυ and converting the slope of the fitted line to such curves [23].

$$\alpha(\upsilon) = \beta \exp(\frac{h\upsilon}{E_U}) \quad (5)$$

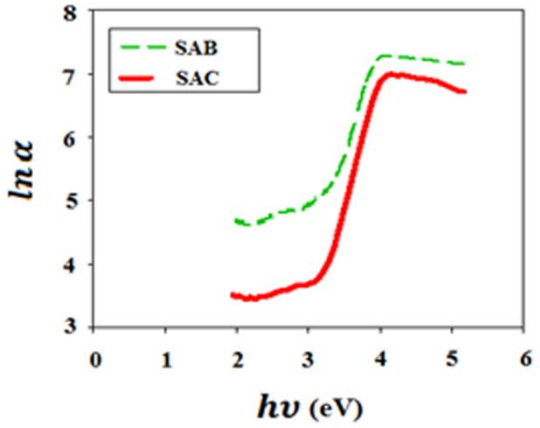

Figure 5. Ln(α) vs. hυ curves for SAC and SAB samples

Figure 5 shows the plots of Ln(α) vs. hυ of samples. Urbach energy of glasses are calculated from these curves and listed in Table. 2. Again lower band tailing energy of SAB implies its higher structural order compared to SAC.

4. CONCLUSIONS

1- According to DTA curves, it sounds like that the crystallization of BaF_2 nanocrystals from SAB glass was more difficult than the crystallization of the CaF_2 nanocrystals from SAC glass.
2- Higher crystallization temperature of BaF_2 in SAB indicated that the network of sample SAB is more continuous than SAC.
3- Lower bandgap energy of direct and indirect bandgaps (2.90 and 3.40 eV, respectively) of SAB glass was evidence of its lower transparency and better semiconducting behavior than SAC glass.
4- Urbach energy calculations also proved the higher degree of order in the SAB network and lower dangling bonds in its structure.
5- From the hardness and semiconducting behavior points of view, the sample SAB was preferred to the glass SAC. Furthermore, it was more favorable than SAC considering the lower mean crystal size of BaF_2 in the crystallized SAB sample. However, the lower transparency of SAB in the UV-Vis region was undeniable.

5. ACKNOWLEDGEMENTS

We would like to show our gratitude to Ali Rahimian and Amin Ahmadi, our colleagues who provided insight and experties that assisted this research.

REFERENCES

1. Poulain, M., Poulain, M., Lucas, J., "Verres fluores au tetrafluorure de zirconium proprietes optiques d'un verre dope au Nd^{3+}", ***Materials Research Bulletin***, Vol. 10, No. 4, (1975), 243-246.
2. Nazabal, V., Poulain, M., Olivier, M., Pirasteh, P., Comy, P., Doualan, J. L., Guy, S., Djouama, T., Boutarfaia, A., Adam, J. L., "Fluoride and oxyfluoride glasses for optical applications", ***Journal of Flourine Chemistry***, Vol. 134, (2012), 18-23.
3. Stevenson, A. J., Serier-Brault, H., Gredin, P., Mortier, M., "Fluoride materials for optical applications: single crystals, ceramics, glasses, and glass-ceramics", ***Journal of Fluorine Chemistry***, Vol. 132, No. 12, (2011), 1165-1173.
4. Babu, P., Jang, K. H., Kim, E. S., Shi, L., Seo, H. J., Lopez, F.E., "Optical properties and white-light emission in Dy^{3+}-doped transparent oxyfluoride glass and glass ceramics containing CaF_2 nanocrystals", ***Journal of the Korean Physical Society***, Vol. 54, No. 4, (2009), 1488-1491.
5. Polishchuk, S.A., Ignat'eva, L.N., Marchenko, Y.V., Bouznik, V.M., "Oxyfluoride glasses (a review)", G***lass Physics and Chemistry***, Vol. 37, No. 1, (2011), 1-20.
6. Wang, Y., Ohwaki, J., "New transparent vitroceramics codoped with Er^{3+} and Yb^{3+} for efficient frequency upconversion", ***Applied physics letters***, Vol. 63, No. 24, (1993), 3268-3270.
7. Kishi, Y., Tanabe, S., "Infrared-to-visible upconversion of rare-earth doped glass ceramics containing CaF_2 crystals", ***Journal of Alloys and Compounds***, Vol. 408–412, (2006), 842–844.
8. Imanieh, M. H., Eftekhari Yekta, B., Marghussian, V., Shakhesi, S., Martín, I. R., "Crystallization of nano calcium fluoride in CaF_2-Al_2O_3-SiO_2 system", ***Solid State Sciences***, Vol. 17, (2013), 76-82.
9. Dejneka, M. J., "The luminescence and structure of novel transparent oxyfluoride glass-ceramics", ***Journal of Non-Crystalline Solids***, Vol. 239, No. 1-3, (1998), 149-155.
10. Antuzevics, A., Kemere, M., Ignatans, R., "Local structure of gadolinium in oxyfluoride glass matrices containing SrF_2 and BaF_2 crystallites", ***Journal of Non-Crystalline Solids***, Vol. 449, (2016), 29–33.

11. Hill, R. G., Goat, C., Wood, D., "Thermal Analysis of a SiO_2-Al_2O_3-CaO-CaF_2 Glass", ***Journal of the American Ceramic Society***, Vol. 75, No. 4, (1992), 778- 785.
12. Fu, J., Parker, J. M., Flower, P. S., Brown, R. M., "Eu^{3+} ions and CaF_2-containing transparent glass-ceramics", ***Materials Research Bulletin***, Vol. 37, No. 11, (2002), 1843-1849.
13. Sung, Y. M., "Crystallization kinetics of fluoride nanocrystals in oxyfluoride glasses", ***Journal of Non-Crystalline Solids***, Vol. 358, No. 1, (2012), 36-39.
14. Rüssel, C., "Nanocrystallization of CaF_2 from $Na_2O/K_2O/CaO/CaF_2/Al_2O_3/SiO_2$ glasses", ***Chemistry of Materials***, Vol. 17, No. 23, (2005), 5843-5847.
15. Rezvani, M., Farahinia, L., "Structure and optical band gap study of transparent oxyfluoride glass-ceramics containing CaF_2 nanocrystals", ***Materials & Design***, Vol. 88, (2015), 252–257.
16. Gautam, C. R., "Synthesis and optical properties of SiO_2–Al_2O_3–MgO–K_2CO_3–CaO–MgF_2–La_2O_3 glasses", ***Bulletin of Materials Science***, Vol. 39, No. 3, (2016), 677-682.
17. Nourbakhsh, Z., Lusk, M., Hashemifar, S. J., Akbarzadeh, H., "Nano structures of amorphous silicon: localization & energy gap", ***Iranian Journal of Physics Research***, Vol. 13, No. 3, (2013), 283 -287.
18. Mott, N. F., Davis, E. A., "Electronic processes in non-crystalline materials", Oxford university press, (2012).
19. Shakeri, M. S., Rezvani, M., "Optical band gap and spectroscopic study of lithium alumino silicate glass containing Y^{3+} ions", ***Spectrochimica Acta Part A: Molecular and Biomolecular Spectroscopy***, Vol. 79, No. 5, (2011), 1920-1925.
20. Lak, F., Rezvani, M., "Optical Characterization of BK7 Borosilicate Glasses Containing Different Amounts of CeO_2", ***Advanced Ceramics Progress***, Vol. 2, No. 3, (2016), 17-24.
21. Rezvani, M., Farahinia, L., "Structure and optical band gap study of transparent oxyfluoride glass-ceramics containing CaF_2 nanocrystals", ***Materials & Design***, Vol. 88, (2015), 252-257.
22. Rosenberg, H. M., "The solid state: an introduction to the physics of crystals for students of physics, materials science, and engineering", 3rd edition, Oxford University press, Oxford, (1988).
23. Abdel-Baki, M., Abdel-Wahab, F. A., Radi, A., El-Diasty, F., "Factors affecting optical dispersion in borate glass systems", ***Journal of Physics and Chemistry of Solids***, Vol. 68, No. 8, (2007), 1457- 1470.